Maintaining quantum coherence in the presence of noise through state monitoring

T. Konrad[1,2,*] and H. Uys[3,†]

[1]*Center for Quantum Technologies, School of Physics, University of KwaZulu, Natal, Durban, South Africa*

[2]*National Institute of Theoretical Physics, Durban, South Africa*

[3]*National Laser Centre, Council for Scientific and Industrial Research, Pretoria, South Africa*

(Received 12 August 2011; published 4 January 2012)

Unsharp measurements allow the estimation and tracking of quantum wave functions in real time with minimal disruption of the dynamics. Here we demonstrate that high-fidelity state monitoring, and hence quantum control, is possible, even in the presence of classical dephasing and amplitude noise, by simulating such measurements on a two-level system undergoing Rabi oscillations. Finite estimation fidelity is found to persist indefinitely after the decoherence times set by the noise fields in the absence of measurement.

DOI: 10.1103/PhysRevA.85.012102 PACS number(s): 03.65.Ta, 03.65.Yz, 05.40.Ca

I. INTRODUCTION

Maintaining high-fidelity quantum control is a central requirement in a variety of technologies ranging from nuclear magnetic resonance to quantum-based precision measurement [1]. Quantum control is usually restricted to a finite time window as a result of the unavoidable influence of decohering environments, and the control lifetime is often extended through the use of decoherence-free subspaces [2], or dynamical decoupling [3].

In this article, we discuss a scheme which maintains quantum control through a sequence of consecutive measurements, of which the corresponding measurement operators form members of a positive operator-valued measure (POVM). We demonstrate that the time evolution of a driven, isolated two-level quantum system, subject to classical dephasing and amplitude noise, can be monitored long beyond its Rabi coherence time. In fact, the wave function can, in principle, be tracked indefinitely with finite fidelity, unlike systems controlled by dynamical decoupling that ultimately undergo complete loss of coherence. The control scheme relies on periodic application of special POVM-measurements said to be "unsharp" in the sense that they are not projective and hence only weakly disturb the dynamics [4]. Such measurements have previously been shown to allow faithful monitoring of Rabi oscillations if the general form of a time-independent Hamiltonian is known [5,6] and no external noise is present.

A scheme for updating a state estimate during continuous measurements [7]—the continuum limit of the technique employed here—has been presented in [8]. In that scheme, the evolving state of the system, as well as an estimate of that state, and the measurement readout are described by three coupled stochastic differential equations, which indicate that the state estimate converges to the real state for a broad class of systems; cf. [9]. Continuous measurements have also been shown to drive statistical mixtures of spatial wave packets into pure states, which can be entirely determined by the measurement record alone [10].

Specific experimental implementations of unsharp measurements have been suggested in the context of Bose-Einstein condensates [11], cavity QED [12], and coupled quantum dots [13,14]. Several realizations of the related topic of "weak-value" measurement have been demonstrated through measurements of photon momentum [15–18]. In addition, experiments of "continuous weak measurement" were implemented using a cold cesium vapor [19]. These realizations all employed ensemble measurements, while here we show monitoring of a single, isolated quantum system by repeated measurement as the system evolves.

II. POVM MEASUREMENT SCHEME

We consider a two-level system undergoing Rabi oscillations. In a frame rotating at the two-level transition frequency, it evolves under the Hamiltonian

$$H_R = \hbar \frac{\Omega_R}{2} \hat{\sigma}_x, \tag{1}$$

where $\hat{\sigma}_x$ is the Pauli matrix that generates rotations about the x axis and Ω_R is the Rabi frequency, which is assumed to be known. At the same time, we assume that the system is under the influence of random classical noise fields $\beta(t)$ and $\alpha(t)$, causing dephasing and amplitude fluctuations, respectively, through a noise Hamiltonian

$$H_N = \hbar\beta(t)\hat{\sigma}_z + \hbar\alpha(t)\hat{\sigma}_x. \tag{2}$$

Each noise field is characterized by a power spectrum, which, by the Wiener-Kintchine theorem, is related to its autocorrelation function

$$C^{(2)}(\tau) = \langle \xi(t)\xi(t+\tau) \rangle \tag{3}$$

through

$$P_\xi(\omega) = \int C^{(2)}(\tau) e^{i\omega\tau} d\tau, \tag{4}$$

where $\xi(t) = \alpha(t), \beta(t)$, and the angle brackets in Eq. (3) indicate an ensemble average.

The estimation strategy rests on carrying out unsharp POVM-measurements periodically [20], and updating the state estimate based on the measurement outcomes. Quite generally, a POVM-measurement with outcome n, which was carried out

*konradt@ukzn.ac.za

†huys@csir.co.za

on a system in the state $|\psi\rangle$, will result in a state after the measurement given by

$$|\psi_n\rangle = \frac{\hat{M}_n|\psi\rangle}{\sqrt{p(n|\psi)}}. \tag{5}$$

Here, $\hat{M}_n$ is the so-called Kraus operator, corresponding to the measurement outcome n, and

$$p(n|\psi) = \langle\psi|\hat{M}_n^\dagger\hat{M}_n|\psi\rangle \tag{6}$$

is the probability to detect outcome n, conditioned on the system being in state $|\psi\rangle$.

In an estimation experiment, a sequence of periodic measurements, with period τ, are applied to the system as it evolves in time [6]. Despite the dynamics, the state change due to the measurement can still be described by Eq. (5) if each measurement is executed much faster than all other dynamical time scales (impulsive measurement approximation). Between measurements, the time evolution is described by the operator

$$\hat{U}_j = \mathcal{T}\left(\exp\left\{-\frac{i}{\hbar}\int_{t_j}^{t_j+\tau}[H_R + H_N(t)]dt\right\}\right), \tag{7}$$

where $\mathcal{T}$ is the time-ordering operator. At $t = N\tau$, after N measurements, the system is, up to the appropriate normalization constant, in the state

$$|\psi(N\tau)\rangle = \hat{M}_{n_N}\hat{U}_N\hat{M}_{n_{N-1}}\hat{U}_{N-1}\ldots\hat{M}_{n_1}\hat{U}_1|\psi\rangle. \tag{8}$$

To estimate the state of the system, the same sequence of operators corresponding to the measured outcomes in Eq. (8) are applied to an initial guess $|\psi_e\rangle$ (cf. [8]), however,

(i) the initial estimate of the state $|\psi_e\rangle$ can be taken as an arbitrary state vector on the Bloch sphere, and

(ii) between measurements, the state estimate is assumed to evolve only through the Hamiltonian given by Eq. (1), since the experimenter does not know what the instantaneous values of the noise fields are.

As we will see in what follows, it is still possible to estimate the state of the system without detailed knowledge of the noise fields. Our approach differs from [5] where the Rabi frequency was assumed to be unknown and one of the aims was to determine its value through a Bayesian estimator in the absence of noise.

We now define two projectors, $\hat{P}_+ = \frac{1}{2}(\mathbb{1} + \hat{\mathbf{r}}\cdot\hat{\sigma})$ and $\hat{P}_- = \frac{1}{2}(\mathbb{1} - \hat{\mathbf{r}}\cdot\hat{\sigma})$, where $\mathbb{1}$ is the identity operator, $\hat{\mathbf{r}} = (\delta,\zeta,\chi)$ is a unit vector on the Bloch sphere, and $\hat{\sigma} = (\hat{\sigma}_x,\hat{\sigma}_y,\hat{\sigma}_z)$. With these terms, it is possible to construct POVM operators $\hat{M}_0 = \sqrt{p_0}\,\hat{P}_+ + \sqrt{1-p_0}\,\hat{P}_-$ and $\hat{M}_1 = \sqrt{1-p_0}\,\hat{P}_+ + \sqrt{p_0}\,\hat{P}_-$, related via $M_0^\dagger M_0 + M_1^\dagger M_1 = \mathbb{1}$ and $0 \leqslant p_0 \leqslant 0.5$. The strength of a single measurement is quantified by $\Delta p = (1-p_0) - p_0 = 1 - 2p_0$ [21]. However, the strength of a sequence of measurements depends also on the period τ between two consecutive measurements. For fixed Δp, a shorter (longer) period τ means a stronger (weaker) influence of the sequential measurement. The strength of the state disturbance due to this sequential measurement is best quantified by the rate $\gamma_m = 1/\tau_m$ with $\tau_m = 2\tau/(\Delta p)^2$ [21]. The strength γ_m is the expected rate at which an arbitrary initial state is reduced to an eigenstate of the measured observable, in the absence of dynamics other than measurement [6].

III. RESULTS AND DISCUSSION

To set the stage, we illustrate the method in the absence of noise, i.e., $\beta(t) = \alpha(t) = 0$. We simulate an experiment in which we choose $\Delta p = 0.2$ and $\hat{\mathbf{r}} = (0,0,1)$, which corresponds to an unsharp measurement of $\hat{\sigma}_z$ (cf. [5]). We carry out a measurement every $\tau = T_R/10$, where $T_R = 2\pi/\Omega_R$ is the Rabi period. The resulting measurement strength is thus smaller than the Rabi frequency ($\gamma_m = \Omega_R/10\pi$), which is required in order not to disturb the oscillations too strongly. For a measurement strength γ_m much greater than Ω_R, the state would be projected onto an eigenstate of the observable $\hat{\sigma}_z$ before a single oscillation could take place, and the dynamics would freeze (similarly to the quantum Zeno effect [22]). The result of each measurement is chosen at random, commensurately with the probabilities prescribed by Eq. (6). The initial-state estimate is chosen orthogonal to the initial-state vector, a limiting case for which the estimation procedure might be expected to have some difficulty.

In Fig. 1(a), we plot the expectation value of $\langle\hat{\sigma}_z\rangle$ for the true state (black line) and the state estimate (red line) for one single run of the measurement experiment. The state (black line) undergoes Rabi oscillations, but with measurement-induced random phase shifts compared to the undisturbed oscillations (dashed blue line). The oscillations, including the influence of the measurement, are monitored accurately by the estimate (red line) after about six Rabi periods. After this time, not only does the expectation value of the measured observable $\hat{\sigma}_z$ with respect to the true and estimated state coincide, but the states themselves also do, as is indicated by the plot of the estimation fidelity, $F(t) = |\langle\psi_{\rm est}|\psi\rangle|^2$, in Fig. 1(b). Asymptotically, the fidelity tends to unity, indicating the perfect state monitoring of a single system, in real time, in the absence of noise.

Now consider a more realistic situation in which the two-level system is not isolated but is subject to random classical noise, as described by the Hamiltonian of Eq. (2).

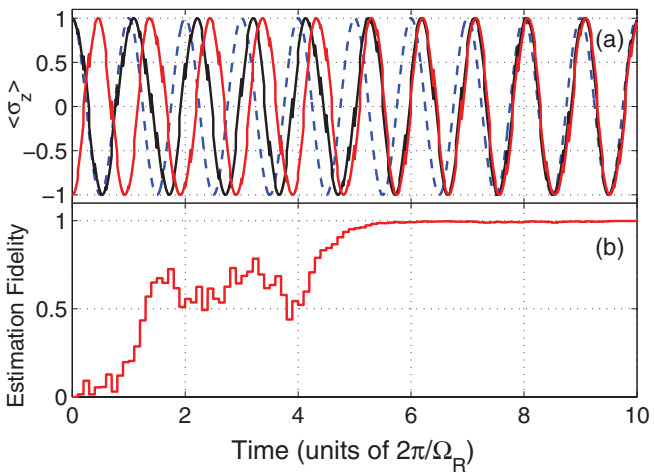

FIG. 1. (Color online) Wave-function estimation in the absence of noise (single run). (a) Expectation value $\langle\hat{\sigma}_z\rangle$ for the true expectation value (black line), estimated expectation value (red, gray line), and expectation value in the absence of measurements (dashed blue line). (b) Estimation fidelity.

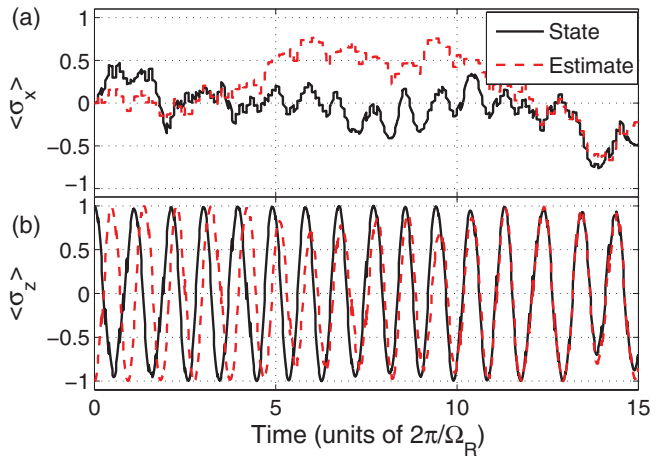

FIG. 2. (Color online) State estimation in the presence of dephasing and amplitude noise. (a) Expectation value of $\hat{\sigma}_x$ and (b) expectation value of $\hat{\sigma}_z$. Here we used $\Delta\beta = 0.05$, $\Delta\alpha = 0.005$, $\Delta p = 0.2$, and $\hat{\mathbf{r}} = (0.43,0,0.9)$.

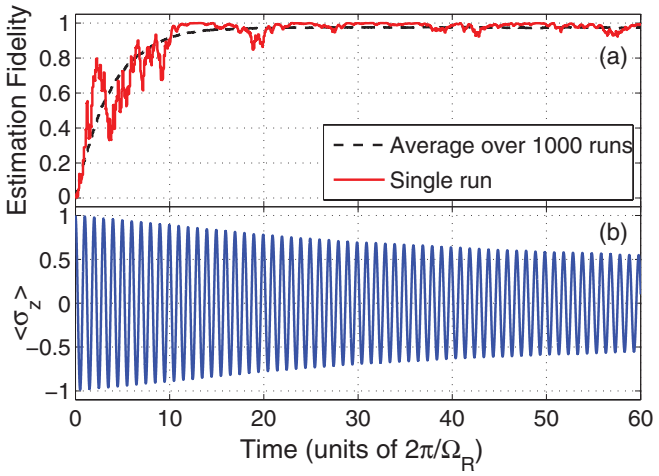

FIG. 3. (Color online) State estimation in the presence of classical noise. (a) Estimation fidelity for a single run (red line), corresponding to Fig. 2; expected fidelity obtained by averaging 1000 runs (dashed black line). (b) Rabi oscillations showing monotonic loss of coherence in the absence of unsharp measurements (blue line).

As an example, we assume that the noise fields both have a power spectrum $P_\xi(\omega) = A_\xi/\omega$, since this "one-over-$f$" noise is ubiquitous in many systems. For concreteness, we choose a lower cutoff of $\omega = 0.01$ and a high-frequency cutoff of $\omega = 10$, where the frequency is specified in units of Ω_R. In accordance with Eqs. (3) and (4), we generate a specific noise trajectory by summing over different spectral components, weighing each with the square root of the noise power: $\xi(t) = \sum_i \sqrt{P_\xi(\omega_i)}\cos(\omega_i t + \phi_i)$. Each spectral component contains a random phase factor ϕ_i, allowed to vary between $[0,2\pi]$, and assumed to be δ correlated. Each noise trajectory, $\alpha(t)$ and $\beta(t)$, is normalized so that their root-mean-square deviations are, respectively, one-hundredth and one-tenth of the drive field amplitude, $\Delta\alpha = 0.005$ and $\Delta\beta = 0.05$. We use the same measurement strength as before, but an observable $\hat{\mathbf{r}}\cdot\hat{\sigma}$ with a finite x component, $\hat{\mathbf{r}} = (0.43,0,0.9)$, since the noise is expected to tip the Bloch vector out of the yz plane.

Figure 2 displays the evolution of the expectation values (a) $\langle\hat{\sigma}_x\rangle$ and (b) $\langle\hat{\sigma}_z\rangle$ for the true state (black lines) and the estimate (red lines), again for a single run of the experiment. The amplitude of the Rabi oscillations, shown in Fig. 2(b), although modulated by the noise, does not decrease permanently and the estimate succeeds in tracking both components. The red line in Fig. 3(a) shows the estimation fidelity corresponding to the single run of the experiment of Fig. (2). Despite the noise, the state estimate quickly approaches the real state, although the fidelity does not converge completely to unity. Instead, it exhibits random excursions away from unity, which at long times are centered around an average, asymptotic value. To find this asymptotic value, we execute 1000 runs of the experiment with the same initial conditions and average over the resulting fidelities, leading to the dashed black curve in Fig. 3(a). We have found empirically that this average fidelity $\bar{F}$ is well described by

$$\bar{F}(t) = F_0(1 - e^{-t/\tau_E}). \tag{9}$$

In Eq. (9), F_0 is the asymptotic estimation fidelity and τ_E is the estimation time. By fitting Eq. (9) to the simulated result, we extract an estimation time of $\tau_E = 3.7T_R$ and an asymptotic fidelity of $F_0 = 0.98$. For comparison, the blue curve in Fig. 3(b) plots the result of an average over 1000 simulated runs of the experiment in the *absence of measurements*, but with the same noise source as in (a). It shows the decay of Rabi oscillations to about half-amplitude over the same time span due to the noise. Labeling τ_R as the characteristic decay time of Rabi oscillations, we remark that Eq. (9) holds accurately only when $\tau_m \ll \tau_R$. For $\tau_m \gtrsim \tau_R$, the asymptotic approach is no longer simply exponential.

The results of Figs. 3(a) and 3(b) taken together imply that in any *single run* of the experiment, the state can be estimated at all times after convergence with an average of 98% fidelity, by a pure state $|\psi_e(t)\rangle$. On the other hand, in the absence of measurements, the state would lose coherence due to the noise, and evolve into a statistical mixture as evidenced by the decay of Rabi oscillations of the ensemble average, as shown in Fig. 3(b). This constitutes the main result of this article. The fidelity can be operationally tested at the end of a run by deducing from the state estimate the appropriate unitary rotations needed to place the system in the state $|\uparrow\rangle$, say, where it will then be detected with 98% probability. As such, the experimenter has maintained quantum control by the monitoring of the state evolution, despite the noise.

Finally, we study the effectiveness of the estimation process as a function of the measurement strength, γ_m, when noise is present. The simulations are repeated for different values of γ_m, and still choosing $\hat{\mathbf{r}} = (0.43,0,0.9)$ in each case. Figures 4(a) and 4(b), respectively, plot the estimation fidelities and convergence times as a function of γ_m for different noise strengths: no noise (diamonds), $\Delta\beta = 0.05$, $\Delta\alpha = 0.005$ (circles), and $\Delta\beta = 0.1$, $\Delta\alpha = 0.01$ (squares). When noise is present, the asymptotic fidelity monotonically decreases as the measurement strength becomes weaker, and approaches

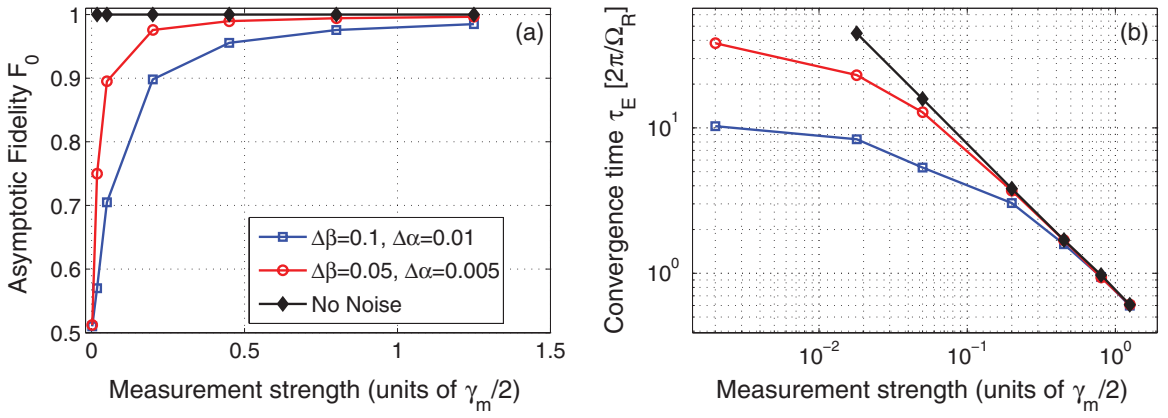

FIG. 4. (Color online) Effect of measurement strength on state estimation in environments with different noise strengths: No noise (diamonds), $\Delta\beta = 0.05$, $\Delta\alpha = 0.005$ (circles), and $\Delta\beta = 0.1$, $\Delta\alpha = 0.01$ (squares). (a) Asymptotic fidelity F_0 as a function of measurement strength. (b) Convergence time τ_E as a function of measurement strength. For the three weakest γ_m's on the curves with noise, we plot in (a) the asymptotic fidelity and in (b) the time that it takes to reach a fraction $1 - e^{-1}$ of that fidelity, even though the corresponding fidelity curves are not strictly exponential.

$F_0 = 0.5$ as $\gamma_m \to 0$. This is consistent with the average fidelity obtained when taking random guesses for the state estimate. Simultaneously, the convergence time increases as the measurement becomes weaker, but plateaus to a finite value as $\gamma_m \to 0$. By contrast, in the absence of noise, the fidelity always approaches $F_0 = 1$, but the convergence time increases indefinitely as the measurement strength weakens, as can be seen in Fig. 4(b).

The trends observed in Fig. 4 emphasize that the appropriate time scales need to be obeyed for the measurement scheme to work. The sequential measurement must be weak enough not to freeze the dynamics, but strong enough to enable a high-fidelity estimate before the noise randomizes the system, i.e., $T_R \ll \tau_m \ll \tau_R$.

IV. CONCLUSION

In conclusion, we remark that this study was carried out in a regime of comparatively strong noise, namely, $\Omega_R/\Delta\beta \sim 5$–$10$. With stronger drive fields, higher asymptotic fidelities can be expected for the same measurement strengths considered here. For example, we find that if $\Omega_R/\Delta\beta = 100$, $\Omega_R/\Delta\alpha = 1000$, $\Delta p = 0.1$, and $\hat{\mathbf{r}} = (0.43,0,0.9)$, then $F_0 = 0.999$ and $\tau = 15.8T_R$. It is encouraging that the estimation procedure described here predicts finite estimation fidelity despite the presence of random classical noise. This opens the way for quantum control techniques that monitor wave-function dynamics beyond the limitations set by decoherence processes in the absence of unsharp measurements.

[1] C. W. Chou, D. B. Hume, J. C. J. Koelemeij, D. J. Wineland, and T. Rosenband, Phys. Rev. Lett. **104**, 070802 (2010).
[2] G. Palma, K. Suominen, and A. Ekert, Proc. R. Soc. London A **452**, 567 (1996).
[3] L. Cywinski, R. M. Lutchyn, C. P. Nave, and S. Das Sarma, Phys. Rev. B **77**, 174509 (2008).
[4] P. Busch, M. Grabowski, and J. Lahti, *Operational Quantum Physics* (Springer Verlag, Heidelberg, 1995).
[5] J. Audretsch, F. Klee, and T. Konrad, Phys. Lett. A **361**, 212 (2007).
[6] J. Audretsch, T. Konrad, and A. Scherer, Phys. Rev. A **63**, 052102 (2001).
[7] V. P. Belavkin, Lecture Notes in Control and Information Science Vol. 121 (Springer-Verlag, Berlin,1989).
[8] L. Diosi, T. Konrad, A. Scherer, and J. Audretsch, J. Phys. A **39**, L575 (2006).
[9] T. Konrad, A. Rothe, F. Petruccione, and L. Diosi, New J. Phys. **12**, 043038 (2010).
[10] A. C. Doherty, S. M. Tan, A. S. Parkins, and D. F. Walls, Phys. Rev. A **60**, 2380 (1999).
[11] J. F. Corney and G. J. Milburn, Phys. Rev. A **58**, 2399 (1998).
[12] J. Audretsch, T. Konrad, and A. Scherer, Phys. Rev. A **65**, 033814 (2002).
[13] A. N. Korotkov, Phys. Rev. B **67**, 235408 (2003).
[14] N. P. Oxtoby, J. Gambetta, and H. M. Wiseman, Phys. Rev. B **77**, 125304 (2008).
[15] N. W. M. Ritchie, J. G. Story, and R. G. Hulet, Phys. Rev. Lett. **66**, 1107 (1991).
[16] P. B. Dixon, D. J. Starling, A. N. Jordan, and J. C. Howell, Phys. Rev. Lett. **102**, 173601 (2009).
[17] O. Hosten and P. Kwiat, Science **319**, 787 (2008).
[18] S. Koksis, B. Braverman, S. Ravets, M. Stevens, R. Mirin, L. Shalm, and A. Stenberg, Science **332**, 1170 (2011).
[19] A. Silberfarb, P. S. Jessen, and I. H. Deutsch, Phys. Rev. Lett. **95**, 030402 (2005).
[20] M. A. Nielsen and I. Chuang, *Quantum Computation and Quantum Information* (Cambridge, United Kingdom, 2002).
[21] J. Audretsch, L. Diósi, and T. Konrad, Phys. Rev. A **66**, 022310 (2002).
[22] B. Misra and E. Sudarshan, J. Math. Phys. **18**, 756 (1977).